PCCP

Accepted Manuscript

ROYAL SOCIETY OF CHEMISTRY

www.rsc.org/pccp

Cite this: DOI: 10.1039/c0xx00000x

www.rsc.org/pccp

PAPER

Anisotropic Electron-Transfer Mobilities in Diethynyl-indenofluorene-diones Crystals as High-Performance n-Type Organic Semiconductor Materials: Remarkable Enhancement by Varying Substituents

Xiao-Yu Zhang,[a,b] Jin-Dou Huang,[b] Juan-Juan Yu,[a] Peng Li,[b] Wei-Ping Zhang*[a] and Thoma Frauenheim*[c]

Received (in XXX, XXX) Xth XXXXXXXXX 20XX, Accepted Xth XXXXXXXXX 20XX
DOI: 10.1039/b000000x

In this study, the electron-transfer properties for the alkynylated indenofluorene-diones of varying substituents (SiMe3, SiPr3, SiPh3) function as n-type organic semiconductors were comparatively investigated at the first-principle DFT level based on the Marcus-Hush theory. The reorganization energies are calculated by adiabatic potential-energy surface method, and the coupling terms are evaluated through a direct adiabatic model. The maximum value of electron-transfer mobility of SiPr3 is 0.485$cm^2V^{-1}s^{-1}$, which appears at the orientation angle of conducting channel on the reference plane a-b near to 172°/352°. The predicted maximum electron mobility value of SiPr3 is nearly 26 times larger than that of SiPh3. This may be attributed to the largest number of intermolecular π-π interactions. In addition, the mobilities in all three crystals show remarkable anisotropic behavior. The calculated results indicate that SiPr3 could be an ideal candidate as a high-performance n-type organic semiconductor material. Our investigations not only give us an opportunity to completely understand the charge transport mechanisms, but also provide a guideline of the materials design for the electronic applications.

1. Introduction

During the last several decades, basic scientific interests and potential applications in cheap, flexible electronic devices have motivated the research in the field of molecular organic materials.[1-5] Conjugated organic materials have attracted enormous interests because of the intrinsic properties. The conjugated hydrocarbons with extended polycyclic frameworks and their heteroatom containing analogues have been applied as organic materials in electronic devices such as organic light-emitting diodes (OLEDs),[6-8] organic field-effect transistors (OFETs),[9-12] and organic solar cells.[13,14] Since the hole (for p-type) or electron (for n-type) transport can be a critical component in a number of organic semiconductors,[15,16] it is more essential for understanding the relationship between the hole or electron transport and molecular packing in crystals. As we know, when the overlap of the intermolecular π orbitals, which are in phase, is maximized, the mobilities of holes or electrons are increased in solid-state organic semiconductors.[17] In the past decades, a lot of efforts have been focused on investigating p-type (hole-transporting) organic semiconductors.[18-29] Some famous representatives of p-type organic semiconductors, such as pentancene[30] and rubrene,[31] have superior charge transport properties.[32] Moreover, it has been reported that pentancene has the highest field-effect hole mobility for thin film transistors.[33,34] In addition, many research groups commit to design the organic semiconductors in pursuit of higher hole mobilities.[35-38] However, much less information about the comparable processing and performance of n-type organic semiconductors is known.[39-40]

To design n-type organic semiconductors, people begin to introduce the electron withdrawing groups, like carbonyls[41] and imine nitrogens,[42-44] into organic semiconductors due to the lower LUMO energy level caused by these electron deficient moieties. Recently, the indenofluorene (IF) framework as one of n-type semiconductors has received considerable attention due to its intrinsic properties such as the planarity of the IF skeleton and the ability of accepting electrons reversibly.[41,45-48] Furthermore, a series of 6,12-bis[(trialkylsilyl)ethynyl]indeno[1,2-b] fluorene-5,11-diones has been synthesized by Rose and his coworkers.[49] Because these molecules are excellent electron-accepting materials elucidated from the electrochemical and photophysical data, we investigate the electron-transport properties of alkynylated IF-diones with varying substituents (SiMe3, SiPr3, SiPh3) based on the experimental crystal structures. The molecular structures are shown in Figure 1. In our study, we not only calculate the electron-transfer reorganization energy and effective electronic coupling, but also present the simulated anisotropic electron-transfer mobilities of these three materials. The electronic anisotropy as an intrinsic property of organic semiconductors has attracted much attention.[50-60] Sundar et al. first found the anisotropic effects in rubrene crystals in 2004.[58] There are various computational studies for the electronic anisotropy based on ab initio or semiemprical quantum chemical methods.[43,51-54] According to Marcus-Hush theory,[61,62] Deng and Han et al. have reported a simple first-principles-based simulation

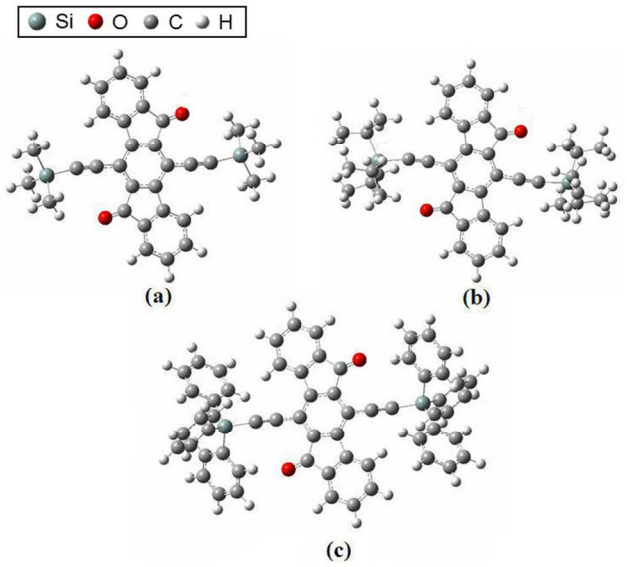

Figure 1. Molecular structures of SiMe3 (a), SiPr3 (b), and SiPh3(c).

model and developed a quantitative function, which shows how the angular resolution anisotropic mobilities correlates with the underlying electronic properties and the molecular packing.[63-65]

In this work, we mainly make a comparative study on the electron-transfer properties of the alkynylated indenofluorene-diones with varying substituents (SiMe3, SiPr3, SiPh3) as n-type organic semiconductors through first-principles calculations, in order to gain insights in the theoretical design of organic transport materials. The calculated results of our theoretical method were in good accordance with the experimental ones for the anisotropic mobility distributions in many organic molecular semiconductors such as linear acene, acene derivates, perylene bisimide derivatives, and oligothiophenes as well as their derivatives /analogues.[66-71] Based on our simulation model, we provide an assessment of the possible range of electron-transfer rates in alkynylated indenofluorene-diones crystals. The analysis is helpful to understand the influence of the structure variations on the transport properties. Our calculations indicate that the SiPr3 crystal could be an ideal candidate as a high-performance n-type organic semiconductor material.

2. Theoretical methods

At room temperature, it is generally accepted that the hole or electron transport in organic semiconductors takes place via charge carrier hopping between neighboring molecules. If we assume no correlation between hopping events and the charge motion is a homogeneous random walk,[36,63,65] the diffusion coefficient caused by the hopping rate is given by eq. (1)

$$D = \lim_{t\to\infty} \frac{1}{2n} \frac{< x(t^2) >}{t} \approx \frac{1}{2n} \sum_i r_i^2 W_i P_i \qquad (1)$$

Where n is the spatial dimensionality, i means the ith pathway, r_i is the intermolecular center-to-center distance of different dimer types, W is the intermolecular hopping rate, and P is the hopping probability, which can be calculated by eq. (2)

$$P_i = \frac{W_i}{\sum_i W_i} \qquad (2)$$

Based the Einstein relation, the drift mobility for charge carrier (hole/electron) transport can be evaluated in organic semiconductors:

$$\mu = \frac{e}{k_B T} D \qquad (3)$$

On the basis of Marcus-Hush theory,[61,62] the hole/electron transport for an organic semiconductors can be described by a hopping mechanism.[36,37,72] The hopping rate (W) can be written as:

$$W = \frac{V^2}{\hbar} \left(\frac{\pi}{\lambda k_B T}\right)^{1/2} \exp\left(-\frac{\lambda}{4 k_B T}\right) \qquad (4)$$

Where V is the effective electronic coupling between neighboring molecules, λ is the reorganization energy, k_B is the Boltzmann constant, and T is the temperature. In these parameters, it indicates that the rate of charge hopping depends on two microscopic parameters: the effective electronic coupling V and the reorganization energy λ. So some efforts have been made to improve the charge mobility of organic semiconductor materials by optimizing these two parameters.[73-75]

Reorganization energy

The reorganization energy usually consists of the internal and external contributions. The internal reorganization energy is caused by relaxation in the molecular geometry, and the external reorganization energy is induced by polarization of the surrounding medium, namely, all the other molecules in the bulk materials. For the organic semiconductors, the contribution from the surrounding molecules to the reorganization energy is very weak and could be neglected because of the very low dielectric constants, so we only consider the internal reorganization energy. The reorganization energy λ in eq. (4) can be evaluated directly using the adiabatic potential energy surface method,[35,76,77] which can be shown as follows:

$$\lambda = \lambda_i^{(1)} + \lambda_i^{(2)} = (E_0^* - E_0) + (E_{+/-}^* - E_{+/-}) \qquad (5)$$

Here, E_0 and $E_{+/-}$ are the energies of the neutral and charged species in their lowest energy geometries, respectively; E_0^* and $E_{+/-}^*$ represent the energies of the neutral and charged species with the geometries of the charged and neutral species, respectively. Figure 2 depicts the sketch of the potential energy surfaces, where $\lambda_i^{(1)}$ corresponds to the geometry relaxation energy of one molecule from neutral state to charged state, and $\lambda_i^{(2)}$ corresponds to the geometry relaxation energy of one molecule from charged state to neutral state.[19,78] This description holds that the $\lambda_i^{(1)}$ and $\lambda_i^{(2)}$ terms are close in energy as long as the potential energy surfaces are harmonic. Then we can calculate the adiabatic ionization potential (IP) and electron affinities (EA) by the following eq.

$$IP = E_+ - E_0 \qquad (6)$$

$$EA = E_- - E_0 \qquad (7)$$

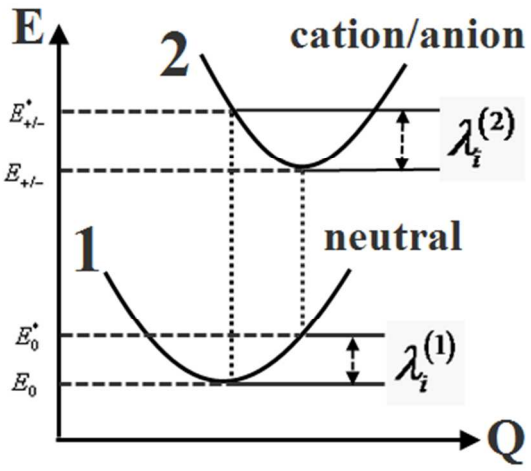

Figure 2. Sketch of the potential energy surfaces for the neutral state and the charged state, showing the vertical transitions (dashed lines).

All geometry optimizations of the monomer molecules both in the neutral and the charged states and the reorganization energy calculations are done at the first-principles DFT level using the B3LYP functional with 6-31G basis set.[79] All the calculations are performed with the Gaussian09 package.[80]

Intermolecular electronic coupling

We choose the method in references 81-83 to calculate the intermolecular electronic coupling of each dimer in organic semiconductors due to the existence of various computational techniques. The geometries for dimer calculations are selected from the observed X-ray crystal structure. The intermolecular electronic coupling (V_{ij}) in eq. (4) can be calculated directly by the spatial overlap (S_{ij}), charge transfer integral (J_{ij}), and site energies (e_i, e_j),[81] which can be written as

$$V_{ij} = \left| \frac{J_{ij} - S_{ij}(e_i + e_j)/2}{1 - S_{ij}^2} \right| \quad (8)$$

For calculating the intermolecular electronic coupling (V_{ij}), we need to calculate the spatial overlap (S_{ij}), charge transfer integral (J_{ij}), and site energies (e_i, e_j):

$$e_{i(j)} = \langle \psi_{i(j)} | H | \psi_{i(j)} \rangle \quad (9)$$

$$S_{ij} = \langle \psi_i | \psi_j \rangle \quad (10)$$

$$J_{ij} = \langle \psi_i | H | \psi_j \rangle \quad (11)$$

where H is the dimer system Kohn-Sham Hamiltonian, and $\Psi_{i(j)}$ represents the monomer HOMOs (for hole transport) or LUMOs (for electron transport) with Löwdin's symmetric transformation, which can be used as the orthogonal basis set for calculation.[83]

All the electronic coupling calculations in different molecular dimers are implemented in the Amsterdam density functional (ADF) program with the local density functional Vosko-Wilk-Nusair (VWN) in conjunction with the PW91 gradient corrections.[82] The TZ2P basis set (the triple-ζ quality including two sets of polarization functions on each atom) was chosen as basis sets throughout the whole process.

Angular resolution anisotropic mobility

The magnitude of the field-effect mobility in a particular transistor channel depends on the specific surface of the organic crystal. Thus, the anisotropic mobility of charge transport in organic semiconductors is an intrinsic property.[58] Han et al. presented a model to simulate the anisotropic mobility (μ_Φ) by projecting the different hopping pathways.[63,65] The equation of angular resolution anisotropic mobility can be given by

$$\mu_\phi = \frac{e}{2k_B T} \sum_i W_i r_i^2 P_i \cos^2 \gamma_i \cos^2(\theta_i - \phi) \quad (12)$$

Where r_i , γ_i and θ_i reflect the intermolecular packing parameters in the organic single crystal. r_i is the ith hopping distance; γ_i is the angle of the ith hopping pathway relative to the transport plane of the organic crystal molecular stacking layer; θ_i and Φ are defined as the orientation angle of the projected electronic coupling pathways of different dimer types and the conducting channel relative to the same reference axis (generally using the crystallographic axis), respectively. So the angles between the different pathways and the conducting channel are θ_i-Φ. P_i and W_i can be calculated by eq. (2) and (4), respectively. For the hopping pathways on the basal transport stacking layer in the organic crystal, the values of γ_i are 0°. Equation (12) provides an analytic function to determine the angular resolution anisotropic mobilities for any type of organic semiconductors by relating the crystal packing and electron coupling V to the outer measuring channel angle Φ.

3. Results and discussion

The geometries of SiMe3, SiPr3, and SiPh3 are full optimized at density functional theory (DFT) with B3LYP/6-31G level to calculate the reorganization energy. Table 1 shows the calculated results of the relaxation energies and reorganization energies in SiMe3, SiPr3, and SiPh3. We compare to the reorganization energies of these three molecules. It can be found clearly that the total reorganization energy of SiPr3 for electron transfer is slightly smaller than those of SiMe3 and SiPh3. Based on the calculated results, we except that SiPr3 would function as more valuable n-type organic semiconductor than SiMe3 and SiPh3 since high reorganization energy is unfavorable for carrier mobilities.[73,84,85] The relative small reorganization energy may be attributed to the expand π-electron conjugation of the triisopropylsilyl (TIPS) substitution on the alkyne terminus.

Table 1 The calculated relaxation energies $\lambda_i^{(1)}$ and $\lambda_i^{(2)}$ as well as reorganization energies λ (in eV).

	Electron transfer		
Molecule	$\lambda_i^{(1)}$	$\lambda_i^{(2)}$	λ
SiMe3	0.1912	0.1854	0.3766
SiPr3	0.1809	0.1747	0.3556
SiPh3	0.2106	0.2137	0.4243

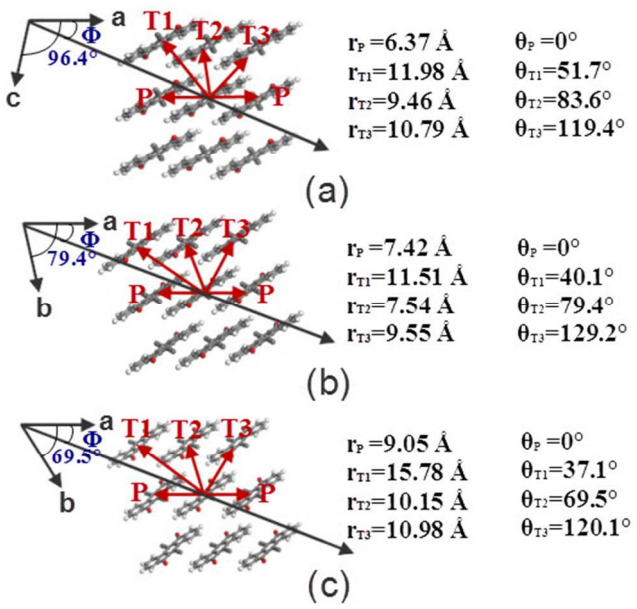

Figure 3. Illustration of charge hopping pathways schemes in SiMe3 (a) and SiPr3 (b) as well as SiPh3 (c) crystals. For ease of viewing, the varying substituents (SiMe3, SiPr3, SiPh3) have been removed since they were oriented similarly in the molecular packing styles, but they were included in all calculations. The X-ray crystal structures are reported previously by Rose et al..[49]

Figure 3 presents the molecular packing styles of SiMe3, SiPr3, and SiPh3 crystals. It can be noted from Figure 3 that all the molecular packing styles of crystal structures exhibit a face-to-face slipped stacking along the a-axis. For these three crystals, we can define four types of intermolecular packing modes as T1, T2, T3, and P. The T1, T2, T3, and P dimers are in the same molecular stacking layer (shown in Figure 3). Since the head-to-tail stacking (L dimer) is out of the molecular stacking layer of T1, T2, T3, and P dimers, we did not discuss the L dimer (out of transport layer plane). The reason is that charge transport in the organic crystals is two dimensional (2D) transport within the stacked layer[86], which means that the charge transport between the layers (L dimer) are less efficient and negligible.

In the discussion of this section, we only considered the interactions of the adjacent neighboring molecules based on the work of Han et al. due to the introduction of nearest-neighbor approximation.[63-66] The intermolecular electronic couplings for electron transport (LUMO) in these four dimers (T1, T2, T3, and P) are calculated based on the local density functional Vosko-Wilk-Nusair (VWN) in conjunction with PW91 gradient corrections and TZ2P basis set, which are listed in Table 2. In addition, the intermolecular center-to-center distances of various packing modes are also summarized in Table 2. It can be seen that the P and T_3 dimers are the most important electron-transport pathways. The electronic couplings V of P and T_3 dimers are much larger than those in other dimers for all three crystals, which indicates that the P and T_3 directions are the dominant conducting channels. This may be attributed to the relatively shorter intermolecular center-to-center distance and larger intermolecular π-π interactions, because the efficient electronic coupling is determined together by these two microscopic parameters. The electronic couplings V of T_1 and T_2 dimers in these three crystals are both very small and negligible. It is noteworthy that the largest electronic couplings for SiPr3 and SiPh3 are 78.15 meV and 18.78 meV at pathway P, but for SiMe3 is 22.57 meV at pathway T_3. Except the case of electronic coupling for SiMe3, the parallel packing mode usually yields larger coupling term than other packings, since the cofacial stacking structure can offer more efficient orbital overlap. Comparing the packing arrangement of SiPr3 with those of SiMe3 and SiPh3, one can find that the distance of T_3 dimers for SiPr3 is 9.55 Å, while those of SiMe3 and SiPh3 are 10.79 and 10.98 Å, respectively. Although there is no significant difference in intermolecular center-to-center distances (10.79 A, 9.55 A and 10.98 A), the T3 dimers of SiPr3 have much larger intermolecular electronic coupling than the counterparts of crystals SiMe3 and SiPh3. This indicates that the electronic coupling is determined not only by the relative intermolecular center-to-center distance but also the orientations of the molecules in dimers. Since the change of relative orientation for molecules in dimers could cause different spatial overlap (S_{ij}) and charge transfer integral (J_{ij}), leading to the change of intermolecular electronic coupling V_{ij} according to the formula (8). For example, the spatial orbital overlap (S_{ij}) and charge transfer integral (J_{ij}) of P dimers in SiPr3 crystal are 14.8 and 131.4 meV. However, the S_{ij} and J_{ij} for T1 dimer in SiPr3 crystal are 0 and 0.01meV, respectively. For the crystals of SiMe3 and SiPh3, the electronic coupling V_p in P dimers are nearly same. Essentially, V_p of SiMe3 crystal is somewhat smaller than that of SiPh3. Notably, although the SiPr3 has a higher intermolecular distance (7.42 Å) than that of SiMe3 (6.37 Å) in the P pathway, the electron coupling of SiPr3 (78.15 meV) is much higher than that of SiMe3 (13.89 meV). This phenomenon can be rationalized from the shape of the lowest unoccupied molecular orbitals (LUMO) of a single molecule and the relative displacements of adjacent molecules along their long molecular axes.[16,76] The packing structures of P dimers and the shapes of LUMO orbitals for SiMe3, SiPr3, SiPh3 are shown in Figure 4. For these three packing structures, there exists a relative displacement of nearly 2.5-3 rings between two parallel molecules. Comparing the shapes of LUMOs for SiMe3, SiPr3 and SiPh3 monomer, almost all the electrons are localized on the alkynylated indenofluorene-diones moiety. In combination with the relative displacement analysis of packing structures, there occurs the compensation of bonding and antibonding interactions between the double bonds of one molecule and the adjacent double bonds of the other molecule for the P dimers of SiMe3

Table 2 Calculated electron-transport electronic couplings V (meV) and intermolecular center-to-center distances r (Å) for the different hopping pathways in SiMe3, SiPr3 and SiPh3 crystals (T=300K).

	SiMe3		SiPr3		SiPh3	
pathways	V	r	V	r	V	r
P	13.89	6.37	78.15	7.42	18.78	9.05
T_1	0.01	11.98	0.010	11.51	0.02	15.78
T_2	0.87	9.46	0.4	7.54	0.28	10.15
T_3	22.57	10.79	44.69	9.55	11.77	10.98

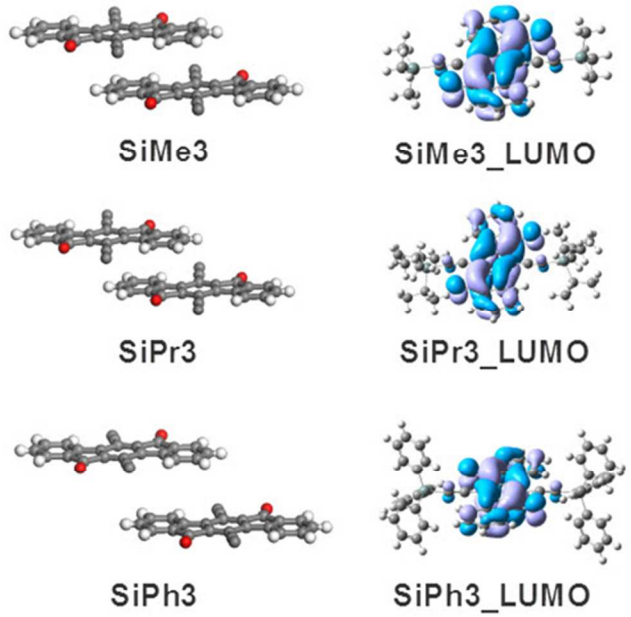

Figure 4. Relative displacements of P dimer along molecule axis and the shapes of LUMOs. For ease of viewing, the varying substituents (SiMe3, SiPr3, SiPh3) have been removed in P dimers because almost all the electrons are localized on the alkynylated indenofluorene-diones moiety.

and SiPh3. That is to say, the relative displacement for SiMe3 and SiPh3 make the positive and negative electron density overlap, which reduces the effective orbital overlap region. However, the relative displacement of P dimer for the SiPr3 expands the π-electron conjugation, which is favorable for carrier mobilities. In summary, it is indicated that the crystal SiPr3 should be more favorable to function as n-type organic semiconductor than the SiMe3 and SiPh3 crystals. The reason may be that the triisopropylsilyl (TIPS) substitution on the alkyne terminus contains the largest number of intermolecular π-π interactions in the solid state.[49] The trialkylsilyl groups uesd, smaller or larger than TIPS, could furnish a variety of crystal-packing motifs that contain fewer π-π interactions.

Figure 3 (a), (b) and (c) show the projecting of various hopping pathways onto a transistor channel in the plane a-c of SiMe3 crystal and plane a-b of SiPr3 crystal as well as plane a-b of SiPh3 crystal, respectively. The crystallographic a axis is set to be the reference axis. The hopping pathways of various dimer types are all on the reference plane, so the angles of γ_i are 0°. The angles between the hopping pathways of P, T_1, T_2, and T_3 dimer types and the reference axis a are labeled as θ_P, θ_{T1}, θ_{T2} and θ_{T3}, respectively. The orientation angle of the conducting channel relative to the reference axis a is Φ. Thus, the angles between the hopping pathways of P, T_1, T_2, T_3 dimer types and the conducting channel are θ_P-Φ, θ_{T1}-Φ, θ_{T2}-Φ and θ_{T3}-Φ. Using the eq. (12) with the calculated reorganization energy λ (in Table 1) and electronic coupling V (in Table 2), the mobility orientation function in the a-c plane for SiMe3 crystal can be written as (a)

$$\mu_{\emptyset} = 0.003cos^2\emptyset + 7.54 * 10^{-16}cos^2(51.7 - \emptyset) + 1.04 * 10^{-17}cos^2(83.6 - \emptyset) + 0.060cos^2(119.4 - \emptyset) \quad (a)$$

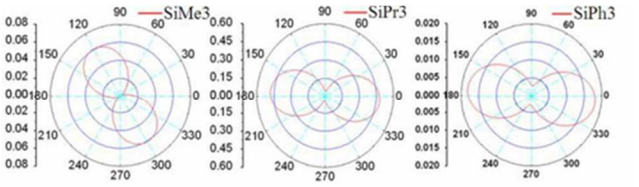

Figure 5. The calculated mobility anisotropy curves of SiMe3, SiPr3, and SiPh3 crystals ($cm^2V^{-1}s^{-1}$). Warning: the scales of each curve are different.

Similarly, the eq. (12) lead to the angular resolution anisotropic mobility orientation functions of SiPr3 and SiPh3 in the a-b basal plane as equation (b) and (c), respectively. The equation (b) and (c) are given as follow

$$\mu_{\emptyset} = 0.447cos^2\emptyset + 2.88 * 10^{-16}cos^2(40.1 - \emptyset) + 4.26 * 10^{-10}cos^2(79.4 - \emptyset) + 0.079cos^2(129.2 - \emptyset) \quad (b)$$

$$\mu_{\emptyset} = 0.017cos^2\emptyset + 6.76 * 10^{-14}cos^2(37.1 - \emptyset) + 1.15 * 10^{-9}cos^2(69.5 - \emptyset) + 0.004cos^2(120.1 - \emptyset) \quad (c)$$

Figure 5 gives the calculated anisotropic electron mobilities of SiMe3, SiPr3, and SiPh3, respectively. For these three crystals, there are not yet reported the angular resolution anisotropic mobility measurements for alkynylated IF-diones with varying substituents (SiMe3, SiPr3, SiPh3). It can be seen clearly that the electron-transfer mobilities in all these three single crystals show remarkable anisotropic behavior. Interestingly, the anisotropic mobility curve of SiPr3 is nearly the same as that of SiPh3 because of their similar crystal structures, however, the electron-transfer mobility of SiPr3 is obviously larger than that of SiPh3, which is about 26 times. As discussed by the article above, it could be caused by the relatively smaller reorganization energy and larger electronic coupling, which are more favorable for carrier mobilities. The highest mobilities of SiPr3 and SiPh3, as 0.485 and 0.018 $cm^2V^{-1}s^{-1}$, appear when the values of Φ are both near to 172°/352°. Different from the crystals SiPr3 and SiPh3, the maximum value (0.060 $cm^2V^{-1}s^{-1}$) of electron mobility for SiMe3 appears when the values of Φ is near to 120°/300°, which may be interpreted as the difference of the reference plane. The simulated mobility values of SiMe3, SiPr3 and SiPh3 crystals in the parallel and perpendicular direction are summarized in Table 3 to compare the anisotropy ratios of electron mobility. The angular-resolution anisotropic mobility analysis shows the importance to control the directions of crystals in applications to improve the material performance. It is indicated that electrons in SiPr3 crystal are intrinsically much more mobile than electrons in SiMe3 and SiPh3 crystals. These differences, which are derived from the relative magnitude of electron-transfer integrals in

Table 3 Simulated electron drift mobility values ($cm^2V^{-1}s^{-1}$) for SiMe3, SiPr3 and SiPh3 crystals in the parallel and perpendicular direction based on equation (12) at room temperature (T=300K).

	Parallel direction		Perpendicular direction	
Crystal	0°	180°	90°	270°
SiMe3	0.017	0.020	0.046	0.045
SiPr3	0.474	0.478	0.045	0.047
SiPh3	0.018	0.018	0.003	0.003

different dimers, can be explained easily based on the mobility orientation function.

4. Conclusions

In this study, we have comparatively investigated the electron-transfer properties for the alkynylated IF-diones with varying substituents (SiMe3, SiPr3, SiPh3) function as n-type organic semiconductors at the first-principles DFT level based on Marcus-Hush theory. We not only calculate the reorganization energies and effective electronic couplings, but also present the simulated anisotropic electron-transfer mobilities of these three materials. The reorganization energies are calculated by the adiabatic potential-energy surface method, and the coupling terms are evaluated through a direct adiabatic model. All the curves of electron-transfer mobility for these three crystals show remarkable anisotropic behavior. Furthermore, the calculated results show that SiPr3 crystal possesses high intrinsic electron-transfer mobilities for using as an ideal n-type organic semiconductor. The maximum value of electron-transfer mobility of SiPr3 is 0.485$cm^2V^{-1}s^{-1}$, which is near 26 times larger than that of SiPh3. Based on these detailed calculations, the conclusion is drawn that the alkynylated IF-diones with the triisopylsilyl (TIPS) substitution on the alkyne terminus have wider application prospects as promising novel n-type organic semiconductor materials, because the TIPS substitution has relatively larger intermolecular π-π interactions. In other words, the use of trialkylsilyl groups, which are smaller or larger than TIPS, could furnish a variety of crystal-packing motifs that contain fewer π-π interactions. It is important that our studies not only offer a reasonable analysis of charge transport properties for the semiconductor materials, but also predict the preferred design of organic electronic devices and provide a guideline for "tailoring" new organic compound for organic electronics to obtain the highest electron mobility performance.

Acknowledgements

This work was supported by the NSFC (2903094 and 20833008) and NKBRSF (2009CB220010 and 2013CB834604).

Notes and references

[a] *School of Materials Science and Engineering, Dalian University of Technology, 2 Linggong Road, Dalian 116024, P. R. China. E-mail: zhang_xy@mail.dult.edu.cn, zhangwp@dlut.edu.cn*
[b] *State Key Laboratory of Molecular Reaction Dynamics, Dalian Institute of Chemical Physics, Chinese Academy of Science, 457 Zhongshan Road, Dalian 116023, P. R. China.*
[c] *Bremen Center for Computational Materials Science, University of Bremen, Am Fallturm 1, D-28359 Bremen, Germany.*

1 H. Sirringhaus, T. Kawase, R. H. Friend, T. Shimoda, M. Inbasekaran, W. Wu, E. P. Woo, *Science* 2000, **290**, 2123.
2 J. A. Rogers, *Science* 2001, **291**, 1502.
3 X. L. Xiao, L. M. Yang, H. Zhao, Z. B. Hu, Y. D. Li, *Nano Res.* 2012, **5**, 27.
4 H. E. Katz, A. J. Lovinger, J. Johnson, C. Kloc, T. Slegrist, W. Li, Y. Y. Lin, A. Dodabalapur, *Nature* 2000, **404**, 478.
5 J. H. Burroughes, D. D. C. Bradley, A. R. Brown, R. N. Marks, K. Mackay, R. H. Friend, P. L. Burns, A. B. Holmes, *Nature* 1990, **347**, 539.
6 G. Barbarella, M. Melucci, G. Sotgiu, *Adv. Mater.* 2005, **17**, 1581.
7 I. F. Perepichka, D. F. Perepichka, H. Meng, F. Wudl, *Adv. Mater.* 2005, **17**, 2281.
8 M. Berggren, O. Inganäs, G. Gaustafsson, J. Rasmusson, M. R. Andersson, T. Hjertberg, O. Wennerstrom, *Nature* 1994, **372**, 444.
9 S. Nagamatsu, K. Kaneto, R. Azumi, M. Matsumoto, Y. Yoshida, K. Yase, *J. Phys. Chem. B* 2005, **109**, 9374.
10 X. Chi, D. Li, H. Zhang, Y. Chen, V. Garcia, C. Garcia, T. Siegrist, *Org. Electron.* 2008, **9**, 234.
11 M. Muccini, *Nature Mater.* 2006, **5**, 605.
12 A. L. Briseno, S. C. B. Mannsfeld, M. M. Ling, S. H. Liu, R. J. Tseng, C. Reese, M. E. Roberts, Y. Yang, F. Wudl, Z. N. Bao, *Nature* 2006, **444**, 913.
13 P. Peumans, A. Yakimov, S. R. Forrest, *J. Appl. Phys.* 2003, **93**, 3693.
14 S. E. Shaheen, C. J. Brabec, N. S. Sariciftci, F. Padinger, T. Fromherz, J. C. Hummelen, *Appl. Phys. Lett.* 2001, **78**, 841.
15 L. L. Chua, J. Zaumseil, J. F. Chang, E. C. W. Ou, P. K. H. Ho, H. Sirringhaus, R. H. Friend, *Nature* 2005, **434**, 194.
16 J. L. Brédas, J. P. Calbert, D. A. Da Silva, J. Cornil, *Proc. Natl. Acad. Sci. U.S.A.* 2002, **99**, 5804.
17 J. E. Anthony, A. Facchetti, M. Heeney, S. R. Marder, X. Zhan, *Adv. Mater.* 2010, **22**, 3876.
18 J. E. Anthony, *Chem. Rev.* 2006, **106**, 5028.
19 S. Chai, S.-H. Wen, K.-L. Han, *Org. Electron.* 2011, **12**, 1806.
20 S. Chai, S.-H. Wen, J.-D. Huang, K.-L. Han, *J. Comput. Chem.* 2011, **32**, 3218.
21 F. Amy, C. Chan, A. Kahn, *Org. Electron.* 2005, **6**, 85.
22 R. K. Chen, X. C. Yang, H. N. Tian, X. N. Wang, A. Hagfeldt, L. C. Sun, *Chem. Mater.* 2007, **19**, 4007.
23 Y. Guo, H. Zhao, G. Yu, C. A. Di, W. Liu, S. Jiang, S. Yan, C. Wang, H. Zhang, X. Sun, X. Tao, Y. Liu, *Adv. Mater.* 2008, **20**, 4835.
24 H. N. Tian, I. Bora, X. Jiang, E. Gabrielsson, K. M. Karlsson, A. Hagfeldt, L. C. Sun, *J. Mater. Chem.* 2011, **21**, 12462.
25 T. Liao, C. H. Sun, Z. Q. Sun, A. J. Du, D. Hulicova-Jurcakova, S. C. Smith, *J. Mater. Chem.* 2012, **22**, 13751.
26 H. H. Dam, F. Caruso, *Adv. Mater.* 2011, **23**, 3026.
27 C. J. Ochs, T. Hong, G. K. Such, J. Cui, A. Postma, F. Caruso, *Chem. Mater.* 2011, **23**, 3141.
28 W. Zhao, Y.-B. Qi, T. Sajoto, S. Barlow, S. R. Marder, A. Kahn, *Appl. Phys. Lett.* 2010, **97**, 123305.
29 C. K. Chan, A. Kahn, *Appl. Phys. A* 2009, **95**, 7.
30 K. Xiao, Y. Q. Liu, T. Qi, W. Zhang, F. Wang, J. H. Gao, W. F. Qiu, Y. Q. Ma, G. L. Cui, S. Y. Chen, X. W. Zhan, G. Yu, J. G. Qin, W. P. Hu, D. B. Zhu, *J. Am. Chem. Soc.* 2005, **127**, 13281.
31 E. Menard, A. Marchenko, V. Podzorov, M. E. Gershenson, D. Fichou, J. A. Rogers, *Adv. Mater.* 2006, **18**, 1552.
32 M. L. Tang, A. D. Reichardt, N. Miyaki, R. M. Stoltenberg, Z. Bao, *J. Am. Chem. Soc.* 2008, **130**, 6064.
33 D. Knipp, R. A. Street, A. Volkel, J. Ho, *J. Appl. Phys.* 2003, **93**, 347.
34 H. Klauk, M. Halik, U. Zschieschang, G. Schmid, W. Radlik, W. Weber, *J. Appl. Phys.* 2002, **92**, 5259.
35 G. R. Hutchison, M. A. Ratner, T. J. Marks, *J. Am. Chem. Soc.* 2005,

127, 2339.
36 W. Q. Deng, W. A. Goddard III, *J. Phys. Chem. B* 2004, **108**, 8614.
37 V. Coropceanu, J. Cornil, D. A. Da Silva Filho, Y. Olivier, R. Silbey, J. L. Brédas, *Chem. Rev.* 2007, **107**, 926.
38 V. Podzorov, V. M. Pudalov, M. E. Gershenson, *Appl. Phys. Lett.* 2003, **82**, 1739.
39 J. A. Letizia, M. R. Salata, C. M. Tribout, A. Facchetti, M. A. Ratner, T. J. Marks, *J. Am. Chem. Soc.* 2008, **130**, 9679.
40 Y. Ie, Y. Umemoto, M. Okabe, T. Kusunoki, K. I. Nakayama, Y. J. Pu, J. Kido, H. Tada, Y. Aso, *Org. Lett.* 2008, **10**, 833.
41 H. Usta, C. Risko, Z. Wang, H. Huang, M. K. Deliomeroglu, A. Zhukhovitskiy, A. Facchetti, T. J. Marks, *J. Am. Chem. Soc.* 2009, **131**, 5586.
42 A. Babel, S. A. Jenekhe, *J. Am. Chem. Soc.* 2003, **125**, 13656.
43 M. Winkler, K. N. Houk, *J. Am. Chem. Soc.* 2007, **129**, 1805.
44 J.-I. Nishida, Naraso; S. Murai, E. Fujiwara, H. Tada, M. Tomura, Y. Yamashita, *Org. Lett.* 2004, **6**, 2007.
45 J. Jacob, S. Sax, T. Piok, E. J. W. List, A. C. Grimsdale, K. M€ullen, *J. Am. Chem. Soc.* 2004, **126**, 6987.
46 Y. Miyata, T. Minari, T. Nemoto, S. Isoda, K. Komatsu, *Org. Biomol. Chem.* 2007, **5**, 2592.
47 T. Hadizad, J. Zhang, Z. Y. Wang, T. C. Gorjanc, C. Py, *Org. Lett.* 2005, **7**, 795.
48 T. Nakagawa, D. Kumaki, J.-i. Nishida, S. Tokito, Y. Yamashita, *Chem. Mater.* 2008, **20**, 2615.
49 B. D. Rose, D. T. Chase, C. D. Weber, L. N. Zakharov, M. C. Lonergan, M. M. Haley, *Org. Lett.* 2011, **13**, 2106.
50 O. Ostroverkhova, D. G. Cooke, F. A. Hegmann, R. R. Tykwinski, S. R. Parkin, J. E. Anthony, *Appl. Phys. Lett.* 2006, **89**, 192113.
51 K. Hannewald, P. A. Bobbert, *Phys. Rev. B* 2004, **69**, 075212.
52 G. A. De Wijs, C. C. Mattheus, R. A. De Groot, T. T. M. Palstra, *Synth. Met.* 2003, **139**, 109.
53 S. W. Yin, Y. F. Lv, *Org. Electron.* 2008, **9**, 852.
54 Y. K. Lan, C. I. Huang, *J. Phys. Chem. B* 2008, **112**, 14857.
55 R. L. Headrick, S. Wo, F. Sansoz, J. E. Anthony, *Appl. Phys. Lett.* 2008, **92**, 063302.
56 C. Reese, Z. Bao, *Adv. Mater.* 2007, **19**, 4535.
57 S. C. B. Mannsfeld, J. Locklin, C. Reese, M. E. Roberts, A. J. Lovinger, Z. Bao, *Adv. Funct. Mater.* 2007, **17**, 1617.
58 V. C. Sundar, J. Zaumseil, V. Podzorov, E. Menard, R. L. Willett, T. Someya, M. E. Gershenson, J. A. Rogers, *Science* 2004, **303**, 1644.
59 M. M. Ling, C. Reese, A. L. Briseno, Z. Bao, *Synth. Met.* 2007, **157**, 257.
60 J. Y. Lee, S. Roth, Y. W. Park, *Appl. Phys. Lett.* 2006, **88**, 252106.
61 R. A. Marcus, *J. Chem. Phys.* 1956, **24**, 966.
62 N. S. Hush, *J. Chem. Phys.* 1958, **28**, 962.
63 S.-H. Wen, A. Li, J.-L. Song, W.-Q. Deng, K.-L. Han, W. A. Goddard III, *J. Phys. Chem. B* 2009, **113**, 8813.
64 S.-H. Wen, W.-Q. Deng, K.-L. Han, *PhysChemChemPhys* 2010, **12**, 9267.
65 K. L. Han, J. D. Huang, S. Chai, S. H. Wen, W. Q. Deng, *Protocol Exchange* 2013, DOI: doi:10.1038/protex.2013.070.
66 S.-H. Wen, W.-Q. Deng, K.-L. Han, *Chem. Commun.* 2010, **46**, 5133.
67 S. Chai, S.-H. Wen, J.-D. Huang, K.-L. Han *J. Comput. Chem.* 2011, **32**, 3218.
68 H.-X. Li, R.-H. Zheng, Q. Shi *Phys. Chem. Chem. Phys.* 2011, **13**, 5642.
69 J.-D. Huang, S.-H. Wen, W.-Q. Deng, K.-L. Han *J. Phys. Chem. B* 2011, **115**, 2140.
70 S. Chai, S.-H. Wen, J.-D. Huang, K.-L. Han *Org. Electron.* 2011, **12**, 1806.
71 J.-D. Huang, S.-H. Wen, K.-L. Han *Chem. Asian J.* 2012, **7**, 1032.
72 G. R. Hutchison, M. A. Ratner, T. J. Marks, *J. Am. Chem. Soc.* 2005, **127**, 16866.
73 M. Kuo, H. Chen, I. Chao, *Chem. Eur. J.* 2007, **13**, 4750.
74 C. L. Wang, F. H. Wang, X. D. Yang, Q. K. Li, Z. G. Shuai, *Org. Electron.* 2008, **9**, 635.
75 H. Moon, R. Zeis, E.-J. Borkent, C. Besnard, A. J. Lovinger, T. Siegrist, C. Kloc, Z. Bao, *J. Am. Chem. Soc.* 2004, **126**, 15322.
76 J.-L. Brédas, D. Beljonne, V. Coropceanu, J. Cornil, *Chem. Rev.* 2004, **104**, 4971.
77 V. Coropceanu, T. Nakano, N. E. Gruhn, O. Kwon, T. Yade, K. Katsukawa, J. L. Brédas, *J. Phys. Chem. B* 2006, **110**, 9482.
78 J. R. Reimers, *J. Chem. Phys.* 2001, **115**, 9103.
79 V. Lemaur, D. A. Da Silva Filho, V. Coropceanu, M. Lehmann, Y. Geerts, J. Piris, M. G. Debije, A. M. Van de Craats, K. Senthilkumar, L. D. A. Siebbeles, J. M. Warman, J. L. Brédas, J. Cornil, *J. Am. Chem. Soc.* 2004, **126**, 3271.
80 M. J. Frisch, G. W. Trucks, H. B. Schlegel, G. E. Scuseria, M. A. Robb, J. R. Cheeseman, J. A. Montgomery, T. Vreven, K. N. Kudin, J. C. Burant, J. M. Millam, S. S. Iyengar, J. Tomasi, V. Barone, B. Mennucci, M. Cossi, G. Scalmani, N. Rega, G. A. Petersson, H. Nakatsuji, M. Hada, M. Ehara, K. Toyota, R. Fukuda, J. Hasegawa, M. Ishida, T. Nakajima, Y. Honda, O. Kitao, H. Nakai, M. Klene, X. Li, J. E. Knox, H. P. Hratchian, J. B. Cross, C. Adamo, J. Jaramillo, R. Gomperts, R. E. Stratmann, O. Yazyev, A. J. Austin, R. Cammi, C. Pomelli, J. W. Ochterski, P. Y. Ayala, K. Morokuma, G. A. Voth, P. Salvador, J. J. Dannenberg, V. G. Zakrzewski, S. Dapprich, A. D. Daniels, M. C. Strain, O. Farkas, D. K. Malick, A. D. Rabuck, K. Raghavachari, J. B. Foresman, J. V. Ortiz, Q. Cui, A. G. Baboul, S. Clifford, J. Cioslowski, B. B. Stefanov, G. Liu, A. Liashenko, P. Piskorz, I. Komaromi, R. L. Martin, D. J. Fox, T. Keith, M. A. Al-Laham, C. Y. Peng, A. Nanayakkara, M. Challacombe, P. M. W. Gill, B. Johnson, W. Chen, M. W. Wong, C. Gonzalez, J. A. Pople, Gaussian09; Gaussian, Inc.: Wallingford, CT, 2004.
81 K. Senthilkumar, F. C. Grozema, F. M. Bickelhaupt, L. D. A. Siebbeles, *J. Chem. Phys.* 2003, **119**, 9809.
82 G. Te Velde, F. M. Bickelhaupt, E. J. Baerends, C. F. Guerra, S. J. A. Van Gisbergen, J. G. Snijders, T. Ziegler, *J. Comput. Chem.* 2001, **22**, 931.
83 E. F. Valeev, V. Coropceanu, D. A. Da Silva, S. Salman, J. L. Brédas, *J. Am. Chem. Soc.* 2006, **128**, 9882.
84 S. Mohakud, A. P. Alex, S. K. Pati, *J. Phys. Chem. C* 2010, **114**, 20436.
85 A. Chandekar, J. E. Whitten, *Synth. Met.* 2005, **150**, 259.
86 V. Coropceanu, J. Cornil, D. A. Da Silva, Y. Olivier, R. Silbey, J. L. Brédas, *Chem. Rev.* 2007, **107**, 2165.